


A non-selective endothelin receptor antagonist bosentan modulates kinetics of bone marrow-derived cells in ameliorating pulmonary hypertension in mice

Taichi Kato^{1,2} , Yoshihide Mitani¹, Masahiro Masuya³, Junko Maruyama⁴, Hirofumi Sawada^{1,5}, Hiroyuki Ohashi¹, Yukiko Ikeyama¹, Shoichiro Otsuki¹, Noriko Yodoya¹, Tsutomu Shinohara^{1,6}, Eri Miyata³, Erquan Zhang⁵, Naoyuki Katayama³, Hideto Shimpo⁷, Kazuo Maruyama⁵, Yoshihiro Komada¹ and Masahiro Hirayama¹

¹Department of Pediatrics, Mie University Graduate School of Medicine, Tsu, Japan; ²Department of Pediatrics, Nagoya University Graduate School of Medicine, Nagoya, Japan; ³Department of Hematology and Oncology, Mie University Graduate School of Medicine, Tsu, Japan; ⁴Department of Clinical Engineering, Suzuka University of Medical Science, Suzuka, Japan; ⁵Department of Anesthesiology, Mie University Graduate School of Medicine, Tsu, Japan; ⁶Department of Pediatrics and Neonatology, Nagoya City University Graduate School of Medicine, Nagoya, Japan; ⁷Department of Thoracic and Cardiovascular Surgery, Mie University Graduate School of Medicine, Tsu, Japan

Abstract

The aim of this study was to investigate whether a dual endothelin receptor antagonist bosentan modulates the kinetics of bone marrow-derived stem cells in inhibiting the development of pulmonary hypertension. Bone marrow chimeric mice, transplanted with enhanced green fluorescent protein (eGFP)-positive bone marrow mononuclear cells, were exposed to hypobaric hypoxia or kept in the ambient air, and were daily treated with bosentan sodium salt or saline for 21 days. After the treatment period, right ventricular pressure was measured and pulmonary vascular morphometry was conducted. Incorporation of bone marrow-derived cells was analyzed by immunohistochemistry. Gene expression and protein level in the lung tissue were evaluated by quantitative real-time PCR and western blotting, respectively. The results showed that, in hypoxic mice, right ventricular pressure and the percentage of muscularized vessel were increased and pulmonary vascular density was decreased, each of which was reversed by bosentan. Bone marrow-derived endothelial cells and macrophages in lungs were increased by hypoxia. Bosentan promoted bone marrow-derived endothelial cell incorporation but inhibited macrophage infiltration into lungs. Quantitative real-time PCR analysis revealed that interleukin 6, stromal cell-derived factor-1, and monocyte chemoattractant protein-1 were upregulated by hypoxia, in which interleukin 6 and monocyte chemoattractant protein-1 were downregulated and stromal cell-derived factor-1 was upregulated by bosentan. Protein level of endothelial nitric oxide synthase (eNOS) in the whole lung was significantly upregulated by hypoxia, which was further upregulated by bosentan. Bosentan modulated kinetics of bone marrow-derived ECs and macrophages and related gene expression in lungs in ameliorating pulmonary hypertension in mice. Altered kinetics of bone marrow-derived stem cells may be a novel mechanism of the endothelin receptor blockade *in vivo* and confer a new understanding of the therapeutic basis for pulmonary hypertension.

Keywords

pulmonary hypertension, endothelin receptor antagonist, bone marrow-derived cell

Date received: 15 January 2020; accepted: 21 March 2020

Pulmonary Circulation 2020; 10(2) 1–9

DOI: 10.1177/2045894020919355

Introduction

Pulmonary arterial hypertension is a progressive and life-threatening disorder with elevated pulmonary vascular

Corresponding author:

Yoshihide Mitani, Department of Pediatrics, Mie University Graduate School of Medicine, 2-174 Edobashi, Tsu, Mie Prefecture 514-8507, Japan.

Email: ymitani@clin.medic.mie-u.ac.jp



Creative Commons Non Commercial CC BY-NC: This article is distributed under the terms of the Creative Commons Attribution-NonCommercial 4.0 License (<http://creativecommons.org/licenses/by-nc/4.0/>) which permits non-commercial use, reproduction and distribution of the work without further permission provided the original work is attributed as specified on the SAGE and Open Access pages (<https://us.sagepub.com/en-us/nam/open-access-at-sage>).

© The Author(s) 2020.
Article reuse guidelines:
sagepub.com/journals-permissions
journals.sagepub.com/home/pul



resistance and ultimately leads to right heart failure and premature death. This disease is characterized by the fibroproliferative lesions composed of endothelial cells (ECs), smooth muscle cells, and inflammatory cells.^{1–4} Although recent progress in treatment results in improvement of prognosis, this disease is not curative.^{5,6} Therefore, novel therapeutic targets must be pursued to improve the outcome of the patients.

In spite of the widespread use of clinically relevant non-selective endothelin receptor antagonists, including bosentan, for this disorder,^{6–10} there is limited understanding of the underlying mechanism of anti-remodeling action of such compounds *in vivo*.^{11–14} Endothelin has been believed to play a pivotal role in the development of pulmonary hypertension (PH) on the basis of cell culture studies using smooth muscle cells, ECs, macrophages, and fibroblasts.¹⁵ Although it was believed that those pulmonary vascular cells originated from the resident cells in the lung, several recent reports demonstrated that bone marrow (BM) stem or progenitor cells contribute to the development of pulmonary vascular disease *in vivo*.^{16–22} However, it is unknown whether bosentan impacts the kinetic of BM-derived stem cells in experimental PH. We therefore investigated how bosentan modulates the kinetics of BM-derived cells in inhibiting the development of pulmonary vascular disease by using BM chimeric mice.

Methods

Animals

Transgenic mice with C57BL/6 background that ubiquitously express eGFP were a generous gift from Dr Masaru Okabe (Osaka University, Osaka, Japan). Wild-type mice with C57BL/6 background were purchased from Charles River Japan (Osaka, Japan). All animals received humane care and protocols for all animal experiments were approved by the animal care committee of Mie University School of Medicine (Medicine-503).

Bone marrow transplantation

Bone marrow transplantation (BMT) was performed according to the previously described method.²³ Briefly, BM cells were harvested from femora and tibiae of eGFP mice. Four- to six-week-old male wild-type C57BL/6 mice were lethally irradiated with a total dose of 9.5 Gy. Four hours later, the recipient mice received two million of unfractionated BM cells by tail vein injection. Then the recipient mice were maintained under sterile condition. Six to eight weeks after the BMT, hematopoietic engraftment was confirmed by flow cytometry using FACSCalibur (BD Biosciences, San Jose, CA) as follows. Peripheral blood was obtained from retroorbital plexus of recipient mice. After the hemolysis with 0.15 M NH₄Cl, the percentage of donor-derived eGFP⁺ cells in B-cell, T-cell, and myeloid lineages were analyzed by staining with Phycoerythrin (PE)-conjugated rat anti-mouse CD45R/B220, PE-

conjugated rat anti-mouse Thy-1.2, and a combination of biotinylated rat anti-mouse Gr-1 and PE-conjugated rat anti-mouse Mac-1, respectively. These antibodies were purchased from BD Biosciences Pharmingen (San Jose, CA).

PH models

Six to eight weeks after BMT, mice were kept in hypobaric hypoxic chamber (0.5 atm) for 21 days to produce PH or were kept in an ambient air. During the entire treatment period, we administered bosentan sodium salt 30 mg/kg/day or similar volume of saline (intraperitoneal (ip)) to chronically hypoxic and normoxic mice.

Hemodynamic measurements, tissue preparation, and assessment of right ventricle hypertrophy

After the treatment period, mice were anesthetized with an ip injection of pentobarbital (50 mg/kg). Then a 27-gauge needle connected to a pressure transducer was percutaneously inserted to right ventricle via subxiphoid approach. Right ventricular pressure was recorded with an amplifier system (AP620G, Nihon Kohden, Tokyo, Japan) and a monitor (polygraph system, Nihon Kohden, Tokyo, Japan). Immediately after the hemodynamic measurement, the trachea and the main pulmonary artery were cannulated under mechanical ventilation (SN-480-7, SHINANO Manufacturing Co., Tokyo, Japan). The lungs were then perfused with phosphate buffered saline (PBS), followed by fixation with 4% paraformaldehyde in PBS via catheters cannulated in trachea and main pulmonary artery at 4°C for three hours. Thereafter, paraformaldehyde was substituted with 30% sucrose in PBS at 4°C for overnight, and subsequently the lungs were embedded in paraffin or Tissue-Tek OCT compound (Sakura Finetek Japan Co., Tokyo, Japan). Right ventricle was dissected from left ventricle and interventricular septum. The weight ratio of right ventricle to left ventricle and interventricular septum was evaluated as an index of right ventricular hypertrophy.

Pulmonary morphometry

We performed pulmonary morphometry as previously described.²⁴ Briefly, paraffin sections of lung (thickness, 4 μm) were incubated with 3% hydrogen peroxide, followed by blocking with 1% bovine serum albumin and 5% goat serum in PBS. Sections were then incubated with anti- α -smooth muscle actin (SMA) (mouse monoclonal 1A4, 1:100, Sigma Aldrich, St Louis, MO) and the site of antigen was visualized by using LSAB2 kit (Dako, Carpinteria, CA). All the vessels accompanying alveolar duct and alveolar wall were analyzed without knowing treatment group. The degree of muscularization in normally non-muscular vessels with the diameter of 25–100 μm were assigned to three groups by circumferential staining with α -SMA: (1) non-muscular (<25% of vessel wall); (2) partially muscular (25–75%); and (3) muscular (>75%). The

percentage of the muscularized vessels was defined as the percentage of partially muscular vessel plus muscular vessel per all vessels in each slide. The numbers of vessels per 100 alveoli was also measured as vascular density.

Immunohistochemistry

For double-labeled immunohistochemistry, tissue cryosections (thickness, 5 μ m) were blocked with 1% bovine serum albumin and 5% donkey serum in PBS, followed by incubation with primary antibody and visualization with Alexa 594-conjugated anti-rabbit (donkey polyclonal A21207, 1:400, Life Technologies, Gaithersburg, MD) or anti-rat immunoglobulin (donkey polyclonal A21209, 1:400, Life Technologies, Gaithersburg, MD). For counter-staining, TOPRO3 (Life Technologies) was used. All the slides were mounted with fluorescent mounting medium (Dako) and viewed by confocal laser microscopy (Fluoview FV1000, Olympus, Tokyo, Japan). Primary antibodies used in this study were anti-CD31 (rat monoclonal MEC13.3, 1:100, BD Pharmingen), anti-macrophages/monocytes (rat monoclonal MOMA-2, 1:100, AbD Serotec, Oxford, UK), Cy3-conjugated anti- α -SMA (mouse monoclonal 1A4, 1:100, Sigma Aldrich, St. Lois, MO), and anti-eNOS (rabbit polyclonal PA1-037, 1:100, Affinity Bioreagents, Golden, CO).

Quantitative real-time polymerase chain reaction

To explore the underlying mechanism of the dynamics of BM-derived cells, we analyzed gene expression in the lung of mice exposed to hypoxia using quantitative real-time polymerase chain reaction (qRT-PCR). Total RNA was extracted from lung homogenates of saline-treated or bosentan-treated, and hypoxia-exposed mice for one day using RNeasy tissue and blood mini kit (Qiagen, Hilden, Germany). The lungs of saline-treated normoxic mice were used as control. One microgram of RNA was reverse transcribed using SuperScript VILO cDNA Synthesis kit (Life Technologies). For qRT-PCR, LightCycler FastStart DNA Master Plus SYBR Green I (Roche Diagnostics, Basel, Switzerland) and Perfect real time primer (Takara Bio, Shiga, Japan) were used with Light Cycler 1.1 (Roche). Hypoxanthine guanine phosphoribosyltransferase (HPRT) was served as a control for all reactions. PCR primers were as follows: interleukin 6 (IL6) MA039013, monocyte chemoattractant protein-1 (MCP1) MA066003, stromal cell-derived factor-1 (SDF1), MA088217, and HPRT MA031262. The protocol of qRT-PCR reaction was as follows: denaturation for 10 min at 95°C, followed by 50 cycles of amplification for 10 s at 95°C and 25 s at 60°C. Amplification specificity was checked using melting curve analysis. The result was analyzed with Roche Molecular Biochemicals Lightcycler software, ver 3 (Roche). Data were normalized by HPRT and were expressed as fold change compared with control group.

Western blot analysis

Lung tissue of saline-treated or bosentan-treated, and hypoxia-exposed mice for one day was homogenized in lysis buffer containing 150 mM NaCl, 0.5% Triton-X, 50 mM Tris, 1 mM ethylene glycol tetraacetic acid (EGTA), 1 mM ethylenediaminetetraacetic acid (EDTA), 1 mM dithiothreitol, phosSTOP (Roche), and complete protease inhibitor cocktail tablet (Roche). The lungs of saline-treated normoxic mice were used as control. The protein concentration was determined by BCA protein assay kit (Thermo Fisher Scientific, Waltham, MA). Thirty micrograms of protein were subjected to SDS-PAGE and transferred onto polyvinylidene difluoride membranes (Life Technologies). After blocking, membranes were probed with mouse anti-eNOS antibody (BD Transduction Lab) or rabbit anti- β -actin (bACT) antibody (Sigma). Horseradish peroxidase (HRP)-conjugated anti-mouse IgG (GE Healthcare) or anti-rabbit IgG (GE Healthcare) were used as secondary antibody. Subsequently, signals were visualized by Western Lightning Plus (Perkin Elmer, Waltham, MA) and detected by LAS-3000 (GE Healthcare Japan, Hino, Japan). The quantitation of protein band density was measured and was normalized to β -actin using Multi-Gauge, ver 3.1 (Fuji Film, Tokyo, Japan).

Statistics

Quantitative data are expressed as means \pm standard errors of means. Differences between groups were compared by one-way ANOVA followed by Bonferroni's multiple comparison test. A value of $P < 0.05$ was considered significant. All data were statistically analyzed using SPSS Statistics version 21 (IBM, Chicago, IL). The authors had full access to the data and take full responsibility for its integrity of the results. All authors have read and agreed to the article as written.

Results

Bosentan ameliorated hypoxia-induced PH

Compared to saline-treated normoxic mice (17.6 ± 0.9 mmHg), right ventricular systolic pressure was increased in saline-treated hypoxic mice (26.6 ± 1.0 mmHg, $P < 0.01$), which was decreased by bosentan (22.9 ± 1.1 mmHg, $P < 0.05$) (Fig. 1a). Compared to saline-treated normoxic mice (0.27 ± 0.01), the weight ratio of right ventricle to left ventricle and interventricular septum (RV/LV + S) was increased in saline-treated hypoxic mice (0.42 ± 0.02 , $P < 0.01$), which was decreased by bosentan (0.35 ± 0.01 , vs saline-treated hypoxic mice, $P < 0.01$) (Fig. 1b). In the morphometric study, in the alveolar duct level, compared to saline-treated normoxic mice ($47.2 \pm 1.2\%$), the percentage of muscularized vessels was increased in saline-treated hypoxic mice ($82.9 \pm 2.7\%$, $P < 0.01$), which was decreased by bosentan ($68.4 \pm 1.4\%$, $P < 0.01$). In the alveolar wall level, compared to saline-treated

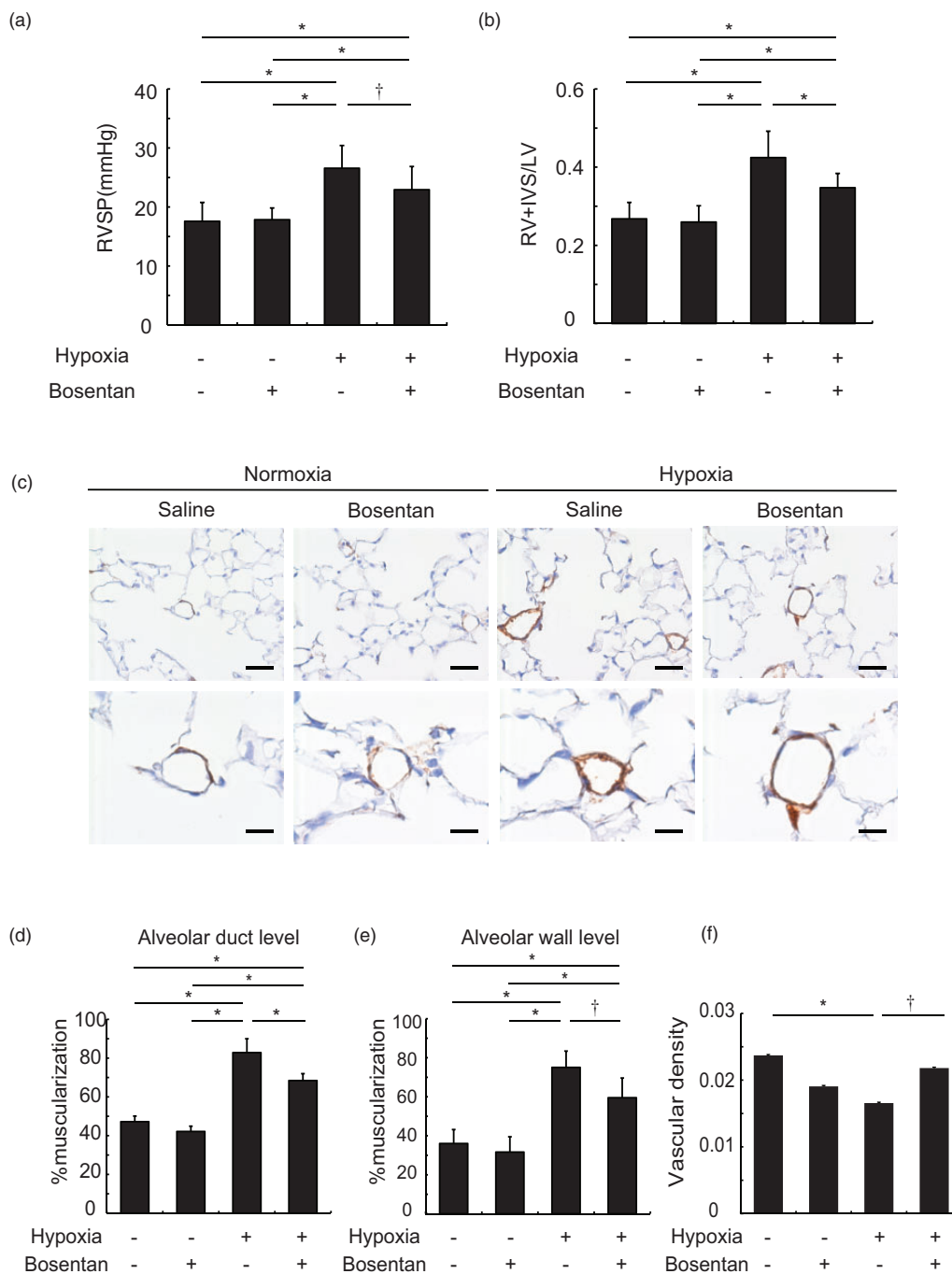


Fig. 1. Bosentan ameliorates hypoxia-induced pulmonary vascular disease in mice. (a and b) Both right ventricular systolic pressure (RVSP) (a) and the weight ratio of right ventricle (RV) to left ventricle (LV) and interventricular septum (IVS) (b) were similarly increased in saline-treated hypoxic mice, which were significantly decreased by bosentan. $n = 12-14$ in each group for RVSP and $n = 9-10$ for the weight ratio; $*P < 0.01$, $\dagger P < 0.05$. (c) Representative immunohistochemistry with α -SMA. Scale bar = 50 μm in upper panels and 20 μm in lower panels. (d and e) In agreement with right ventricular systolic pressure and right ventricular hypertrophy, the percentage of muscularized pulmonary vessels was increased in saline-treated hypoxic mice, which was significantly decreased by bosentan in both alveolar duct level (d) and alveolar wall level (e). $n = 6-7$ in each group; $*P < 0.01$, $\dagger P < 0.05$. (f) Vascular density in the lung was significantly decreased by hypoxia, which was significantly increased by bosentan. $n = 6$ in each group; $*P < 0.01$, $\dagger P < 0.05$.

normoxic mice ($36.1 \pm 2.9\%$), the percentage of muscularized vessels was increased in saline-treated hypoxic mice ($75.0 \pm 3.2\%$, $P < 0.01$), which was decreased by bosentan ($59.5 \pm 3.8\%$, $P < 0.05$) (Fig. 1c-e). Compared to saline-

treated normoxic mice (0.024 ± 0.001), pulmonary vascular density was significantly decreased in the saline-treated hypoxic mice (0.017 ± 0.001 , $P < 0.01$), which was restored by bosentan (0.022 ± 0.001 , $P < 0.05$) (Fig. 1f).

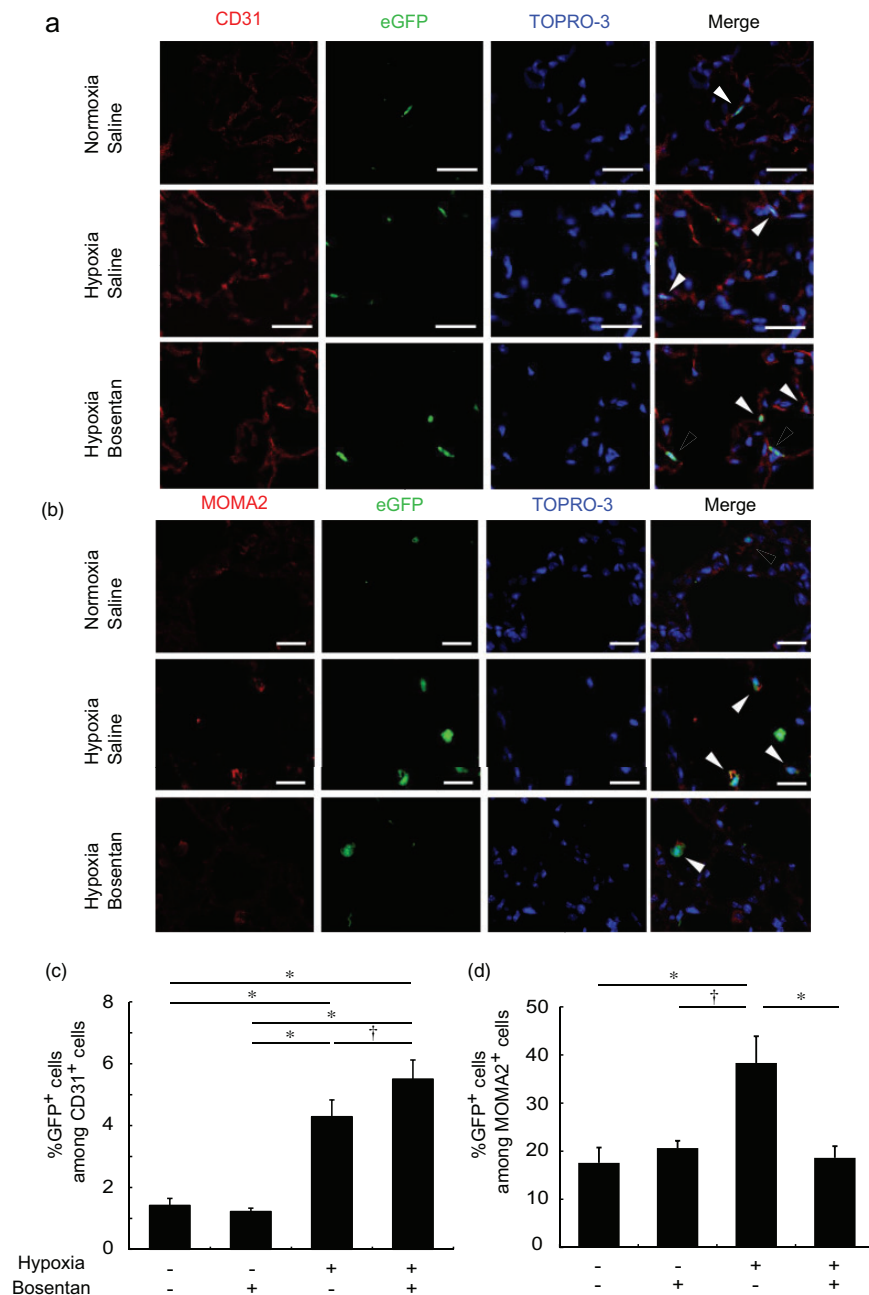


Fig. 2. Bosentan increased BM-derived ECs but inhibited BM-derived macrophages in hypoxia-induced pulmonary vascular disease in mice. (a) Representative confocal laser scanning imaging of CD31⁺, eGFP⁺ BM-derived ECs in saline-treated normoxic mice, saline-treated hypoxic mice, and bosentan-treated hypoxic mice. Scale bar = 25 μ m. Arrowheads indicate CD31⁺ eGFP⁺ BM-derived ECs. (b) Representative confocal laser scanning imaging of MOMA2⁺, eGFP⁺ BM-derived macrophages in saline-treated normoxic mice, saline-treated hypoxic mice, and bosentan-treated hypoxic mice. Scale bar = 25 μ m. Arrowheads indicate MOMA2⁺, eGFP⁺ BM-derived macrophages. (c) BM-derived ECs were significantly increased in saline-treated hypoxic mice compared to saline-treated normoxic mice, which was further increased by bosentan. $n = 3-4$ in each group; * $P < 0.01$, † $P < 0.05$. (d) BM-derived macrophages were significantly increased in saline-treated hypoxic mice compared to saline-treated normoxic mice, which was inhibited by bosentan. $n = 4-6$ in each group; * $P < 0.01$.

Bosentan modulated dynamics of BM-derived ECs and macrophages in pulmonary vascular lesion

The hematopoietic engraftment of transplanted BM-derived cells was confirmed in peripheral blood, six to eight weeks after the BMT (Fig. S1). The double-labeled

immunohistochemical study showed that CD31⁺, eGFP⁺ BM-derived ECs were located in pulmonary capillary vessels. Compared to saline-treated normoxic mice ($1.42 \pm 0.13\%$), the percentage of CD31⁺, eGFP⁺ cells among CD31⁺ cells was increased in saline-treated hypoxic mice ($4.29 \pm 0.31\%$, $P < 0.01$), which was further increased by

bosentan ($5.50 \pm 0.31\%$, $P < 0.05$) (Fig. 2a and c). Compared to saline-treated normoxic mice ($17.4 \pm 2.6\%$), the percentage of MOMA2⁺, eGFP⁺ BM-derived macrophages among MOMA2⁺ macrophages in the pulmonary adventitia was increased in saline-treated hypoxic mice ($38.4 \pm 5.5\%$, $P < 0.01$), which was decreased by bosentan ($18.6 \pm 2.4\%$, $P < 0.01$) (Fig. 2b and d). However, α -SMA⁺, eGFP⁺ BM-derived smooth muscle cells were not found in any sections in the all four groups (Fig. S2). The endothelial phenotype of the

BM-derived CD31⁺ cells was confirmed by eNOS expression in an immunohistochemical study (Fig. S3).

Bosentan modulated gene expression in lung

Compared to saline-treated normoxic mice, mRNA expression levels of SDF1 were up-regulated in saline-treated hypoxic mice, which was further upregulated by bosentan significantly ($P < 0.05$) (Fig. 3a). In contrast, upregulated

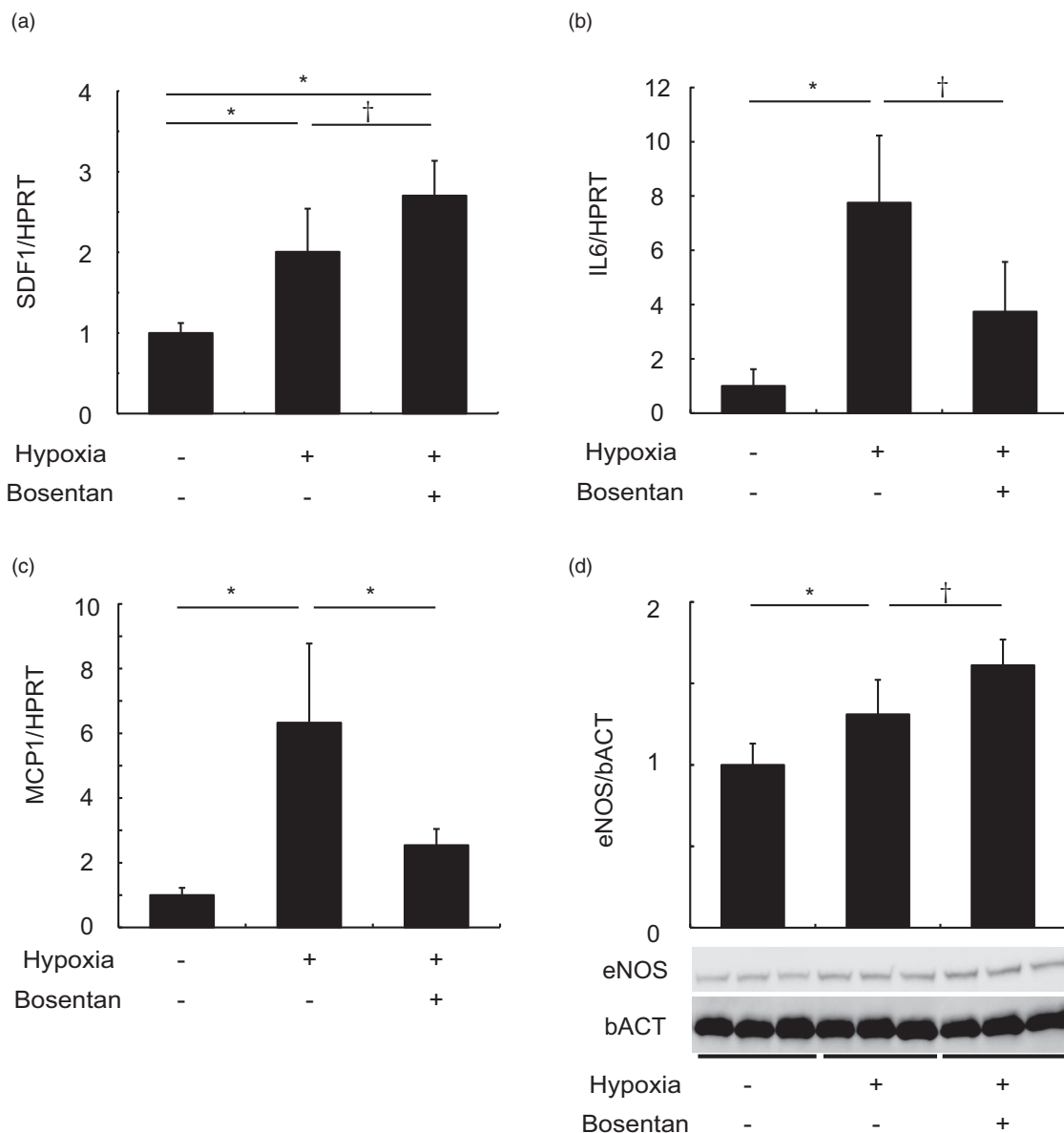


Fig. 3. Bosentan modulated gene expression in lung. (a–c) In saline-treated hypoxic mice, gene expression of SDF1 (a), IL6 (b), and MCP1 (c), determined by real-time PCR, were upregulated compared to saline-treated normoxic mice. On the other hand, in bosentan-treated hypoxic mice, SDF1 was upregulated while both IL6 and MCP1 were downregulated compared to saline-treated hypoxic mice. $n = 4–6$ in each group for SDF1 and $n = 5–6$ in each group for IL6 and MCP1; * $P < 0.01$, † $P < 0.05$. (d) Protein level of eNOS in the whole lung detected by western blotting was significantly upregulated by hypoxia, which was further upregulated by bosentan. $n = 6$ in each group; * $P < 0.01$, † $P < 0.05$. SDF1: stromal cell-derived factor-1; HPRT: hypoxanthine guanine phosphoribosyltransferase; IL6: interleukin 6; MCP1: monocyte chemoattractant protein-1.

mRNA levels of IL6 and MCP1 in saline-treated hypoxic mice were decreased by bosentan (Fig 3. b and c). Increased protein levels of eNOS in saline-treated hypoxic mice were further upregulated by bosentan ($P < 0.05$) (Fig. 3d).

Discussion

The present study demonstrated that in ameliorating pulmonary vascular disease, bosentan increased the recruitment of BM-derived ECs and decreased that of macrophages in the lungs, which was associated with the upregulated expression of SDF1 and eNOS and downregulation of IL-6 and MCP1. These findings suggest that altered BM-derived cell kinetics may be a novel mechanism of action of a clinically useful compound bosentan *in vivo* and confer a new understanding of the therapeutic basis for this disorder.

Although previous studies showed that bosentan inhibited proliferation of pulmonary arterial smooth muscle cells and improved tube formation capacity of pulmonary arterial ECs in cell culture studies.²⁵⁻²⁷ The information related to the mechanisms by which bosentan inhibits pulmonary vascular disease *in vivo*, specifically how bosentan modulated BM-derived stem cells in ameliorating pulmonary vascular disease, was limited.^{11,12,14} We newly demonstrated *in vivo* that bosentan increased BM-derived ECs and decreased BM-derived macrophages in lungs in ameliorating pulmonary vascular disease in mice. Besides vasodilation effect of bosentan, how bosentan's effect of BM-derived cell modulation involved in the improvement of pulmonary vascular disease is unknown. Since exogenous administration of endothelial progenitor cells ameliorated monocrotaline-induced PH in rats and BM-chimeric wild-type mice with BMPR2-disrupted macrophages had aggravated pulmonary vascular disease,^{22,28} it is possible that the impact of bosentan *in vivo* may be mediated at least in part by

modulating BM-derived ECs and/or macrophages, as well as the direct effects on resident vascular smooth muscle cells, ECs, and macrophages in lungs.^{25-27,29}

Furthermore, in the present study, bosentan-induced modulation of BM-derived vascular cells was associated with the upregulated expression of SDF1 and eNOS and downregulation of IL-6 and MCP1. The precise mechanism how bosentan modulated the gene expression *in vivo* and the specificity for endothelin receptors in the modulation of gene expression remain to be determined. Previous report demonstrated that selective ET_A receptor blocker partially reversed Rho kinase-mediated vasoconstriction in blood perfused lungs of a rat PH model.³⁰ The activation of Rho kinase results in upregulation of IL-6 and MCP1 in vascular smooth muscle cells.^{31,32} On the other hand, endothelin downregulates eNOS expression via ET_B receptor in ECs.³³ In addition, bosentan is reported to abrogate the inhibition of eNOS expression by endothelin in ECs.³⁴ Furthermore, the activation of eNOS/Nitric oxide (NO) pathway results in upregulation of SDF1 in the ischemic brain model and myocardial ischemia/reperfusion model.^{35,36} The expression of SDF1 has positive effects on incorporation of the BM-derived ECs in peripheral wound model,³⁷ whereas IL-6 and MCP1 contribute to macrophage accumulation of pulmonary vascular disease.^{38,39} Taken together, it is possible that bosentan promoted BM-derived cells by upregulation of SDF1, which resulted from the upregulation of eNOS through blocking ET_B receptor, and suppressed macrophage accumulation to pulmonary vascular lesion by downregulation of IL-6 and MCP1 through blocking ET_A receptor in this model as summarized in a schematic diagram (Fig. 4).

In conclusion, a clinically used endothelin receptor antagonist bosentan has a novel mechanism *in vivo* mediated by BM-derived cell in inhibiting PH, which may confer a new understanding of the therapeutic basis for this disorder.

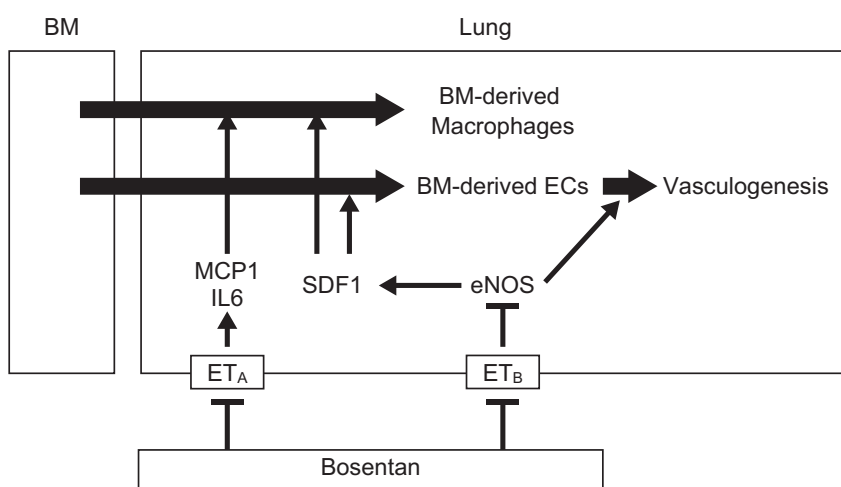


Fig. 4. Summary of the present study. Proposed mechanisms of pharmacomodulation of BM-derived cells by bosentan are shown with the present findings.

BM: bone marrow; EC: endothelial cell; MCP1: monocyte chemoattractant protein-1; IL6: interleukin 6; SDF1: stromal cell-derived factor.

Conflict of interest

TK received speaking honoraria from Actelion Pharmaceuticals and Nippon Shinyaku. YM received speaking honoraria and manuscript fee from Actelion Pharmaceuticals and declares that bosentan sodium salt was gifted from Actelion Pharmaceuticals, Allschwil, Switzerland. HO received research grant from Actelion Pharmaceuticals.

Funding

This work was supported by a grant from the Ministry of Education, Culture, Sports, Science, and Technology (16591023 for Y. M., 23591565 for H. S., 24791057 for N. Y., 936472 for E. Z., 978159 for K. M.) and Grants-in-Aid for Scientific Research from the Japan Society for the Promotion of Science (25460951 and 16K09307 for M. M). The funders had no role in study design, data collection and analysis, decision to publish, or preparation of the manuscript.

ORCID iD

Taichi Kato  <https://orcid.org/0000-0001-7084-4565>

Supplemental material

Supplemental material for this article is available online.

References

- Rabinovitch M. Molecular pathogenesis of pulmonary arterial hypertension. *J Clin Invest* 2012; 122: 4306–4313.
- Guignabert C, Tu L, Girerd B, et al. New molecular targets of pulmonary vascular remodeling in pulmonary arterial hypertension: importance of endothelial communication. *Chest* 2015; 147: 529–537.
- Sawada H, Saito T, Nickel NP, et al. Reduced BMPR2 expression induces GM-CSF translation and macrophage recruitment in humans and mice to exacerbate pulmonary hypertension. *J Exp Med* 2014; 211: 263–280.
- Otsuki S, Sawada H, Yodoya N, et al. Potential contribution of phenotypically modulated smooth muscle cells and related inflammation in the development of experimental obstructive pulmonary vasculopathy in rats. *PLoS One* 2015; 10: e0118655.
- Benza RL, Miller DP, Barst RJ, et al. An evaluation of long-term survival from time of diagnosis in pulmonary arterial hypertension from the REVEAL Registry. *Chest* 2012; 142: 448–456.
- Barst RJ, McGoon MD, Elliott CG, et al. Survival in childhood pulmonary arterial hypertension: insights from the registry to evaluate early and long-term pulmonary arterial hypertension disease management. *Circulation* 2012; 125: 113–122.
- Rubin LJ, Badesch DB, Barst RJ, et al. Bosentan therapy for pulmonary arterial hypertension. *N Engl J Med* 2002; 346: 896–903.
- Galie N, Beghetti M, Gatzoulis MA, et al. Bosentan therapy in patients with Eisenmenger syndrome: a multicenter, double-blind, randomized, placebo-controlled study. *Circulation* 2006; 114: 48–54.
- Humbert M, Sitbon O, Chaouat A, et al. Survival in patients with idiopathic, familial, and anorexigen-associated pulmonary arterial hypertension in the modern management era. *Circulation* 2010; 122: 156–163.
- Tamura Y, Kumamaru H, Satoh T, et al. Effectiveness and outcome of pulmonary arterial hypertension-specific therapy in Japanese patients with pulmonary arterial hypertension. *Circ J* 2017; 82: 275–282.
- Hamidi SA, Lin RZ, Szema AM, et al. VIP and endothelin receptor antagonist: an effective combination against experimental pulmonary arterial hypertension. *Respir Res* 2011; 12: 141.
- Rafikova O, Rafikov R, Kumar S, et al. Bosentan inhibits oxidative and nitrosative stress and rescues occlusive pulmonary hypertension. *Free Radic Biol Med* 2013; 56: 28–43.
- Shinohara T, Sawada H, Otsuki S, et al. Macitentan reverses early obstructive pulmonary vasculopathy in rats: early intervention in overcoming the survivin-mediated resistance to apoptosis. *Am J Physiol Lung Cell Mol Physiol* 2015; 308: L523–L538.
- Gien J, Tseng N, Seedorf G, et al. Endothelin-1-Rho kinase interactions impair lung structure and cause pulmonary hypertension after bleomycin exposure in neonatal rat pups. *Am J Physiol Lung Cell Mol Physiol* 2016; 311: L1090–L1100.
- Dupuis J and Hoeper MM. Endothelin receptor antagonists in pulmonary arterial hypertension. *Eur Respir J* 2008; 31: 407–415.
- Zhao YD, Courtman DW, Deng Y, et al. Rescue of monocrotaline-induced pulmonary arterial hypertension using bone marrow-derived endothelial-like progenitor cells: efficacy of combined cell and eNOS gene therapy in established disease. *Circ Res* 2005; 96: 442–450.
- Satoh K, Kagaya Y, Nakano M, et al. Important role of endogenous erythropoietin system in recruitment of endothelial progenitor cells in hypoxia-induced pulmonary hypertension in mice. *Circulation* 2006; 113: 1442–1450.
- Sahara M, Sata M, Morita T, et al. Diverse contribution of bone marrow-derived cells to vascular remodeling associated with pulmonary arterial hypertension and arterial neointimal formation. *Circulation* 2007; 115: 509–517.
- Spees JL, Whitney MJ, Sullivan DE, et al. Bone marrow progenitor cells contribute to repair and remodeling of the lung and heart in a rat model of progressive pulmonary hypertension. *FASEB J* 2008; 22: 1226–1236.
- Launay JM, Hervé P, Callebert J, et al. Serotonin 5-HT_{2B} receptors are required for bone-marrow contribution to pulmonary arterial hypertension. *Blood* 2012; 119: 1772–1780.
- Amsellem V, Lipskaia L, Abid S, et al. CCR5 as a treatment target in pulmonary arterial hypertension. *Circulation* 2014; 130: 880–891.
- Yan L, Chen X, Talati M, et al. Bone marrow-derived cells contribute to the pathogenesis of pulmonary arterial hypertension. *Am J Respir Crit Care Med* 2016; 193: 898–909.
- Miyata E, Masuya M, Yoshida S, et al. Hematopoietic origin of hepatic stellate cells in the adult liver. *Blood* 2008; 111: 2427–2435.
- Kishimoto Y, Kato T, Ito M, et al. Hydrogen ameliorates pulmonary hypertension in rats by anti-inflammatory and antioxidant effects. *J Thorac Cardiovasc Surg* 2015; 150: 645.e3–654.e3.
- Kunichika N, Landsberg JW, Yu Y, et al. Bosentan inhibits transient receptor potential channel expression in pulmonary vascular myocytes. *Am J Respir Crit Care Med* 2004; 170: 1101–1107.

26. Yamanaka R, Otsuka F, Nakamura K, et al. Involvement of the bone morphogenetic protein system in endothelin- and aldosterone-induced cell proliferation of pulmonary arterial smooth muscle cells isolated from human patients with pulmonary arterial hypertension. *Hypertens Res* 2010; 33: 435–445.
27. Gien J, Tseng N, Seedorf G, et al. Endothelin-1 impairs angiogenesis in vitro through Rho-kinase activation after chronic intrauterine pulmonary hypertension in fetal sheep. *Pediatr Res* 2013; 73: 252–262.
28. Yip HK, Chang LT, Sun CK, et al. Autologous transplantation of bone marrow-derived endothelial progenitor cells attenuates monocrotaline-induced pulmonary arterial hypertension in rats. *Crit Care Med* 2008; 36: 873–880.
29. Gamze K, Mehmet HM, Deveci F, et al. Effect of bosentan on the production of proinflammatory cytokines in a rat model of emphysema. *Exp Mol Med* 2007; 39: 614–620.
30. Oka M, Homma N, Taraseviciene-Stewart L, et al. Rho kinase-mediated vasoconstriction is important in severe occlusive pulmonary arterial hypertension in rats. *Circ Res* 2007; 100: 923–929.
31. Funakoshi Y, Ichiki T, Shimokawa H, et al. Rho-kinase mediates angiotensin II-induced monocyte chemoattractant protein-1 expression in rat vascular smooth muscle cells. *Hypertension* 2001; 38: 100–104.
32. Ito T, Ikeda U, Shimpo M, et al. HMG-CoA reductase inhibitors reduce interleukin-6 synthesis in human vascular smooth muscle cells. *Cardiovasc Drugs Ther* 2002; 16: 121–126.
33. Dong F, Zhang X, Wold LE, et al. Endothelin-1 enhances oxidative stress, cell proliferation and reduces apoptosis in human umbilical vein endothelial cells: role of ETB receptor, NADPH oxidase and caveolin-1. *Br J Pharmacol* 2005; 145: 323–333.
34. Ramzy D, Rao V, Tumiati LC, et al. Elevated endothelin-1 levels impair nitric oxide homeostasis through a PKC-dependent pathway. *Circulation* 2006; 114: I319–I326.
35. Cui X, Chen J, Zacharek A, et al. Nitric oxide donor upregulation of stromal cell-derived factor-1/chemokine (CXC motif) receptor 4 enhances bone marrow stromal cell migration into ischemic brain after stroke. *Stem Cells* 2007; 25: 2777–2785.
36. Li N, Lu X, Zhao X, et al. Endothelial nitric oxide synthase promotes bone marrow stromal cell migration to the ischemic myocardium via upregulation of stromal cell-derived factor-1alpha. *Stem Cells* 2009; 27: 961–970.
37. Gallagher KA, Liu ZJ, Xiao M, et al. Diabetic impairments in NO-mediated endothelial progenitor cell mobilization and homing are reversed by hyperoxia and SDF-1 alpha. *J Clin Invest* 2007; 117: 1249–1259.
38. Savale L, Tu L, Rideau D, et al. Impact of interleukin-6 on hypoxia-induced pulmonary hypertension and lung inflammation in mice. *Respir Res* 2009; 10: 6.
39. Ikeda Y, Yonemitsu Y, Kataoka C, et al. Anti-monocyte chemoattractant protein-1 gene therapy attenuates pulmonary hypertension in rats. *Am J Physiol Heart Circ Physiol* 2002; 283: H2021–H2028.